High nitrogen isotope fractionation of nitrate during denitrification in four forest soils and its implications for denitrification rate estimates

Ang Wang[a, f, g], Yunting Fang[a, f*], Dexiang Chen[b*], Oliver Phillips[c], Keisuke Koba[d], Weixing Zhu[a, e], Jiaojun Zhu[a, f]

[a] CAS Key Laboratory of Forest Ecology and Management, Institute of Applied Ecology, Chinese Academy of Sciences, Shenyang, 110164, China

[b] Research Institute of Tropical Forestry, Chinese Academy of Forestry, Guangzhou 510520, China

[c] School of Geography, University of Leeds, Leeds, UK

[d] Center for Ecological Research, Kyoto University, Shiga, 520-2113, Japan

[e] Department of Biological Sciences, Binghamton University, The State University of New York, Binghamton, NY 13902, USA

[f] Qingyuan Forest CERN, Chinese Academy of Sciences, Shenyang, 110016, China

[g] College of Resources and Environment, University of Chinese Academy of Sciences, Beijing, 100049, China

***Corresponding authors**

Yunting Fang, Institute of Applied Ecology, Chinese Academy of Sciences, 72 Wenhua Road, Shenyang, China 110016. Tel: +86-24-83970302. E-mail: fangyt@iae.ac.cn

Dexiang Chen, Research Institute of Tropical Forestry, Chinese Academy of Forestry, Guangzhou 510520, China. E-mail: dexiangchen@ritf.ac.cn

Abstract

Denitrification is a major process contributing to the removal of nitrogen (N) from ecosystems, but its rate is difficult to quantify. The natural abundance of isotopes can be used to identify the occurrence of denitrification and has recently been used to quantify denitrification rates at the ecosystem level. However, the technique requires an understanding of the isotopic enrichment factor associated with denitrification, which few studies have investigated in forest soils. Here, soils collected from two tropical and two temperate forests in China were incubated under anaerobic or aerobic laboratory conditions for two weeks to determine the N and oxygen (O) isotope enrichment factors during denitrification. We found that at room temperature (20 °C), NO_3^- was reduced at a rate of 0.17 to 0.35 μg N g^{-1} h^{-1}, accompanied by the isotope fractionation of N ($^{15}\varepsilon$) and O ($^{18}\varepsilon$) of 31‰ to 65‰ (48.3 ± 2.0‰ on average) and 11‰ to 39‰ (18.9 ± 1.7‰ on average), respectively. The N isotope effects were, unexpectedly, much higher than reported in the literature for heterotrophic denitrification (typically ranging from 5‰ to 30‰) and in other environmental settings (e.g., groundwater, marine sediments and agricultural soils). In addition, the ratios of $\Delta\delta^{18}O$:$\Delta\delta^{15}N$ ranged from 0.28 to 0.60 (0.38 ± 0.02 on average), which were lower than the canonical ratios of 0.5 to 1 for denitrification reported in other terrestrial and freshwater systems. We suggest that the isotope effects of denitrification for soils may vary greatly among regions and soil types and that gaseous N losses may have been overestimated for terrestrial ecosystems in previous studies in which lower fractionation factors were applied.

Keywords: denitrification; N-isotope fractionation; O-isotope fractionation; $\Delta\delta^{18}O$:$\Delta\delta^{15}N$; forest soils; gaseous N losses

1 Introduction

Nitrogen (N) is an essential element that limits primary production in many forest ecosystems (Vitousek and Howarth, 1991). Anthropogenic emissions of reactive N from fossil fuel combustion and modern agriculture have greatly increased the amount of N deposition into the environment (Gruber and Galloway, 2008). The increased input of N has caused an N excess in certain terrestrial ecosystems, leading to soil acidification and changes in ecosystem structure and function. In soil, denitrification (the stepwise reduction of NO_3^- to NO_2^-, NO, N_2O and N_2) has long been considered a major process of N removal. However, this process is poorly resolved in N cycling studies (Vitousek and Howarth, 1991) because the rate is difficult to quantify at the ecosystem level due to limitations associated with conventional methods, including the intrusive nature of soil sampling, uncertainties in scaling up from local measurements, and the high background N_2 concentration (Groffman et al., 2006).

The natural abundance of stable isotope ratios of nitrogen ($^{15}N/^{14}N$) and oxygen ($^{18}O/^{16}O$) in nitrate (NO_3^-) have been used to evaluate the sources of and biogeochemical transformations acting on NO_3^- (Granger and Wankel, 2016). Microbial denitrifiers exert a large isotope discrimination against ^{15}N and ^{18}O during denitrification, such that the remaining NO_3^- is simultaneously enriched in ^{18}O and ^{15}N at a ratio from 0.5 to 1 (henceforth referred to as $\Delta\delta^{18}O{:}\Delta\delta^{15}N$) (Granger and Wankel, 2016; Kendall et al., 2007; Wunderlich et al., 2012). Thus, the $^{15}N/^{14}N$ and $^{18}O/^{16}O$ ratios in NO_3^- have been used to detect denitrification. The degree of discrimination expressed by the isotope effect, ε, is defined as $\varepsilon = ({}^{light}k / {}^{heavy}k - 1)$ (reported in per mil, ‰). Recently, the $^{15}N/^{14}N$ ratio has been used to quantify denitrification rates at the ecosystem level (Fang et al., 2015; Houlton and Bai, 2009; Houlton et al., 2006). Based on the ^{15}N enrichment in soil and water, including those

of total dissolved N, bulk soil N and NO_3^-, several studies have suggested that denitrification is much more important than previously thought, accounting for 24% to 86% of total N losses (denitrification plus nitrate leaching) from unmanaged terrestrial ecosystems such as forests (Fang et al., 2015; Houlton and Bai, 2009; Houlton et al., 2006).

However, the use of ^{15}N natural abundance to quantify denitrification rates and to constrain N transformation relies heavily on detailed knowledge of the denitrification process and the isotope fractionation involved. The N isotope effect ($^{15}\varepsilon$) varies greatly with environmental and experimental conditions and has been reported to range from 5‰ to 40‰ in pure culture studies of heterotrophic denitrifying bacteria (Barford et al., 1999; Dabundo, 2014; Delwiche and Steyn, 1970; Frey et al., 2014; Granger et al., 2008; Hosono et al., 2015; Karsh et al., 2012; Knöeller et al., 2011; Kritee et al., 2012; Treibergs and Granger, 2016; Wunderlich et al., 2012) and in open ocean systems (Brandes et al., 1998; Cline and Kaplan, 1975; Sigman et al., 2005; Sigman et al., 2003; Voss et al., 2001), from 0‰ to 18‰ in continental sediments (Brandes and Devol, 1997; Brandes and Devol, 2002; Dähnke and Thamdrup, 2015; Kessler et al., 2014), from 5‰ to 30‰ in groundwater (Aravena and Robertson, 1998; Böttcher et al., 1990; Fukada et al., 2003; Lehmann et al., 2003; Mariotti et al., 1988; Mengis et al., 1999; Smith et al., 1991; Vogel et al., 1981; Wenk et al., 2014), and from 2‰ to 50‰ in agricultural soils (Blackmer and Bremner, 1977; Chien et al., 1977; Grabb et al., 2017; Lewicka-Szczebak et al., 2014; Lewicka-Szczebak et al., 2015; Mariotti et al., 1981; Mariotti et al., 1982; Mathieu et al., 2007; Well and Flessa, 2009). Estimations of the denitrification rate at the ecosystem level are sensitive to $^{15}\varepsilon$, and assigning different $^{15}\varepsilon$ values results in different denitrification rates. For example, when the average $^{15}\varepsilon$ of 20‰ from a pure culture of denitrifying bacteria was used,

denitrification was estimated to account for 28% of N loss from unmanaged terrestrial ecosystems; however, when a $^{15}\varepsilon$ of 16‰ was observed for several native soil denitrifier communities, the denitrification contribution increased to 36% (Houlton and Bai, 2009).

Despite numerous studies of the N isotope effect performed using pure cultures of heterotrophic denitrifying bacteria (Granger et al., 2008; Treibergs and Granger, 2016, and references therein), groundwater (Lehmann et al., 2003; Wenk et al., 2014, and references therein), sediments (Dähnke and Thamdrup, 2015; Kessler et al., 2014, and references therein), and agricultural soils (Grabb et al., 2017; Lewicka-Szczebak et al., 2014; Lewicka-Szczebak et al., 2015; Mariotti et al., 1982; Mathieu et al., 2007; Well and Flessa, 2009), only four studies have examined forest soils (Houlton et al., 2006; Menyailo and Hungate, 2006; Perez et al., 2006; Snider et al., 2009). Furthermore, there is no report on the dynamics of the coupled N and O isotope trajectory during denitrification for forest soils via direct measurements of the N- and O-isotopes of NO_3^-. In addition, different environments have different slopes of $\Delta\delta^{18}O{:}\Delta\delta^{15}N$; when plotting $\delta^{18}O$ over $\delta^{15}N$ of the residual NO_3^-, a range from 0.47 to 0.89 was found in terrestrial environments and freshwater systems (Böttcher et al., 1990; Fukada et al., 2003; Lehmann et al., 2003; Wenk et al., 2014), a value of 1.25 in marine environments (Sigman et al., 2005), and a range from 0.33 to 1.02 in pure cultures of heterotrophic denitrifying bacteria (Dabundo, 2014; Frey et al., 2014; Granger et al., 2008; Hosono et al., 2015; Karsh et al., 2012; Knöeller et al., 2011; Kritee et al., 2012; Treibergs and Granger, 2016; Wunderlich et al., 2012). Thus, it is critical to determine the coupled N- and O-isotope discrimination in forest soils during denitrification.

To advance our understanding of isotopic fractionation during denitrification in

forest soils and reduce the uncertainty in denitrification estimates, in this study, we selected four forest soils—two from temperate forests and two from tropical forests—to investigate the isotope fractionation of N and O of NO_3^- during denitrification by native soil microbial communities as well as the relationship between N and O isotopes ($\Delta\delta^{18}O$:$\Delta\delta^{15}N$).

2 Methods and materials

2.1 Study sites

Our two tropical forest ecosystems, a primary forest (PF, 18°43'47"N, 108°53' 23"E, 893 m a.s.l.) and a secondary forest (SF, 18°44'41"N, 108°50'57"E, 935 m a.s.l.), are located in the Jianfengling (JFL) National Natural Reserve (Chinese Ecosystem Research Network, CERN) on Hainan Island, southern China. The tropical forests have a tropical monsoon climate with an annual precipitation of 2,449 mm (more than 80% of which falls during May to October) and an annual average temperature of 19.8 °C (Chen et al., 2010). The primary forest has never been disturbed by human activities and is dominated by Mallotus hookerianus, Gironniera subaequalis, Cryptocarya chinensis and Cyclobalanopsis patelliformis. The soil is an acidic (pH = 4.2) lateritic yellow soil, and the soil texture is sandy clay with 57.1% sand, 18.2% silt, and 24.7% clay (Fang et al., 2004; Luo et al., 2005). The secondary forest was developed on a clear-cut site (1960-1970s) dominated by Castanopsis tonkinensis, S*chefflera octophylla*, Psychotria rubra and Blastus cochinchinensis. The soil is an acidic (pH = 4.1) lateritic yellow soil, and the soil texture is loamy clay with 53.8% sand, 12.1% silt, and 34.1% clay (Fang et al., 2004; Luo et al., 2005).

The two temperate forests, a larch forest dominated by Larix olgensis (LF, 41°50'58"N, 124°56'18"E, 625 m a.s.l.) and a mixed forest (MF, 41°50'48"N, 124°56'01"E, 640 m a.s.l.), are both located in the Qingyuan (QY) Forest (CERN) in

northeastern China. The temperate forests have a continental temperate monsoon climate with an annual precipitation of 811 mm (with more than 80% falling during June, July and August) and an annual average temperature of 4.7 °C (Zhu et al., 2007). The mixed forest was developed from a clear-off following a large fire (1950s) and is dominated by Quercus mongolica, Juglans mandshurica and Phellodendron amurense. The larch forest is a 44-year-old stand dominated by Larix olgensis. The two temperate forests have acidic (pH = 5.2) brown soils and soil texture is clay loam with 25.6% sand, 51.2% silt, and 23.2% clay (Yang et al., 2010).

2.2 Soil sampling and laboratory incubation

In May 2015, we collected 0-10 cm mineral soil from all four forests. In each forest, we established three plots (20 m × 20 m) randomly, and the soils collected from individual plots (six cores taken at six random locations in each plot) were composited into one soil sample (defined as plot-level composite soil), such that we collected three plot-level composite soils for each forest. In May 2016, we resampled soils from the same plots of the tropical primary forest and the temperate mixed forest using the same method. The soils were placed in sterile plastic bags, sealed and transported to the laboratory in the Jianfengling or Qingyuan research stations on ice. In the laboratory, soil was passed through a 2-mm-mesh sieve to remove roots and other visible fragments. For each soil sample, one part was used for incubation and another was used for later analysis of NH_4^+ and NO_3^- concentrations. Subsamples of the soil were also air dried for the analysis of total C and N concentrations.

In 2015, four forest-level composite soils (i.e., three plot-level composite soils in each forest were combined into one forest-level composite soil) were incubated in the laboratory. For each forest soil, we prepared 17 glass vials (50 mL, Chromacol, 125×20-CV-P210); two were used for the measurement of initial conditions, and 15

were used for incubation (i.e., five replicates for each sampling day). For the 15 replicate glass vials, approximately 10 g fresh soil was added to each vial and then amended with 4 mL 3.57 mmol L^{-1} $NaNO_3$ (equal to addition of 20 μg N g^{-1} soil) and 0.1 mL 5% dicyanodiamine (DCD, a nitrification inhibitor), which was prepared using N_2-purged sterile deionized water. The final soil moisture in each vial was adjusted to exceed 100% of the water-filled pore space (WFPS). DCD was used to inhibit nitrifying bacteria to minimize the effect of NO_3^- produced from nitrification. The vials were immediately capped tightly with grey butyl septa (Chromacol, 20-B3P, No. 1132012634) and aluminium crimp seals (ANPEL Scientific Instrument (Shanghai) Co. Ltd., 6G390150). Each vial was vacuumed and flushed with ultra-high-purity He for 5 min (100 mL min^{-1}) so that the soil was under strictly anaerobic conditions. The vials were shaken gently, and the resulting soil slurries were incubated at 20 °C for 3, 7, 14 days. The incubation was terminated by injecting 0.5 mL of a 7 M $ZnCl_2$ solution. Five vials at each sampling day were removed to analyse the NO_3^- concentration and the ^{15}N and ^{18}O abundance of residual NO_3^-.

In 2016, two forest-level composite soils (collected in 2016) were further selected to test the effect of initial NO_3^- concentration, DCD presence and O_2 presence in the headspace on the N and O isotopes. The incubations used methods similar to those used in 2015, with the exception that vials received different treatments, as follows: (A) Initial NO_3^- concentration. Soil samples were divided into three parts: one part was amended with 4 mL 3.57 mmol L^{-1} $NaNO_3$ (equivalent to an addition of 20 μg N g^{-1} soil), one part was amended with 4 mL 1.79 mmol L^{-1} $NaNO_3$ (equivalent to an addition of 10 μg N g^{-1} soil), and one part was amended with 4 mL deionized water (control). Then, the vials were incubated under strictly anaerobic conditions at 20 °C as described above. (B) DCD and O_2 presence. Soil samples were divided into

four parts: two parts were amended with 0.1 mL 5% DCD and incubated under anaerobic or aerobic conditions, and the other two parts were left without DCD and incubated under anaerobic or aerobic conditions. Then, the vials were incubated at 20 °C as described above. The soil samples collected in 2016 were also incubated at 4 ^{o}C under anaerobic conditions, and compared with those incubated at 20 °C to evaluate the effect of incubation temperature. However, NO_3^- was consumed slowly at 4 °C (only 7%-25% of the initial NO_3^-), preventing a valid isotope fractionation calculation (Fig. S1). Although the valid isotope fractionation could not be calculated, the results of $^{15}\varepsilon$ at 4 °C can be found in Table S3. In addition, in 2016, three plot-level composite soils from each forest were incubated using the same method. There were three replicates at each sampling for each treatment. Details of these treatments are provided in Tables 1 and 2.

The soils before and after incubation were extracted with 2 M KCl solution in a soil/solution ratio of 1:4. The KCl was pre-combusted at 450 °C for 48 h, and NO_3^-, NO_2^- and NH_4^+ were not detected in the KCl solution. Ammonium concentrations in the extracts were determined using the indophenol blue method followed by colourimetry. Nitrate concentrations were determined after hydrazine sulfate reduction to nitrite (NO_2^-), followed by diazamine coincidence spectrophotometry. Nitrite concentrations were determined using diazamine coincidence spectrophotometry. All analyses were performed on a Smartchem instrument 200 (Westco Scientific Instruments, Inc., Italy) (Buffen et al., 2014; Talbot et al., 2014). Air-dried soils were used to determine total N and C concentrations using a Vario micro-elemental analyser (Elementar Analysen systeme GmbH, Germany). Soil pH was determined with a glass electrode in a 1:2.5 soil/water suspension. Soil water content was calculated according to the weight change after drying for 24 h at 105 °C.

2.3 Isotope analysis

The air-dried soils were ball milled and analysed for C and N concentrations and $\delta^{15}N$ using an elemental analyser (Elementar Analysen Systeme GmbH, Germany) coupled to an isotope ratio mass spectrometer (Elementar Analysen Systeme GmbH, Germany; IsoPrime100, IsoPrime Limited, UK). Calibrated DL-alanine ($\delta^{15}N$ = -1.7‰), glycine ($\delta^{15}N$ = 10.0‰), and histidine ($\delta^{15}N$ = -8.0‰) were used as internal standards to correct for $\delta^{15}N$ analysis. The analytical precision for $\delta^{15}N$ was 0.2‰. The $\delta^{15}N$ of the sample relative to the standard (atmospheric N_2) was expressed as following:

$$\delta^{15}N = (({}^{15}N/{}^{14}N)_{sample}/ ({}^{15}N/{}^{14}N)_{standard} -1) *1000.$$

Concentrations of residual NO_3^- in soils were measured using the method described above. The N and O isotopic compositions of residual NO_3^- were determined using the modified azide method (Tu et al., 2016). Briefly, Cd powder was used to reduce NO_3^- to NO_2^-, and then NO_2^- was reduced to N_2O by HN_3. The produced N_2O was determined using an automated purge and cryogenic trap system coupled to isotope ratio mass spectrometer (PT-IRMS), which included a continuous-flow IRMS (IsoPrime100, IsoPrime Limited, UK) and a 112-slot auto-sampler (Gilson GX-271, IsoPrime Limited, UK) with a cryo-focusing unit (Trace Gas Preconcentrator, IsoPrime Limited, UK). In our study, the N_2O peak of the reagent blank was approximately 4% of the standards (Table S1). To eliminate the influence of the reagent blank and any drift during IRMS isotope analysis, four standards (IAEA-NO-3, USGS32, USGS34 and USGS35) were used to correct for samples according to the mixing model (Tu et al., 2016) (Table S1, Fig. S2). According to this modified method, the analytical precision of the $\delta^{15}N$ and $\delta^{18}O$ values was 0.2‰ and 0.5‰, respectively.

In addition, for the 2016 incubation with different initial NO_3^- concentrations, we transferred the headspace gas using a gas-tight syringe to a newly vacuumed vial after incubation was terminated by injecting 0.5 mL 7 M $ZnCl_2$ solutions. Then, the $\delta^{15}N$-N_2O in the headspace gas was determined via the same automated PT-IRMS. The $\delta^{15}N$ of the sample was relative to the standard (atmospheric N_2). We used ambient N_2O to correct the $\delta^{15}N$-N_2O for samples ($\delta^{15}N$ of ambient N_2O was determined to be 8.2‰ in our laboratory (the laboratory air was collected and the $\delta^{15}N$ of N_2O was determined with an automated PT-IRMS, as with the incubated samples) while the average value reported was 6.7‰) (Harris et al., 2017; Kim and Craig, 1990).

2.4 Calculation of isotope fractionation

Estimates of N- and O-isotope effects ($^{15}\varepsilon$ and $^{18}\varepsilon$, respectively) were calculated by fitting the $\delta^{15}N$ and $\delta^{18}O$ of NO_3^- to the following linear equations (Mariotti et al., 1981):

$$\delta^{15}N = \delta^{15}N_{initial} - {}^{15}\varepsilon \ln([NO_3^-] / [NO_3^-]_{initial}) \quad (1);$$

$$\delta^{18}O = \delta^{18}O_{initial} - {}^{18}\varepsilon \ln([NO_3^-] / [NO_3^-]_{initial}) \quad (2).$$

We found that in some cases, during the incubation, NO_3^- was almost completely consumed after several days, with its concentration later increasing slightly, and both the ^{15}N and ^{18}O abundance of the remaining NO_3^- substantially decreased. This observation was also reported in previous studies (Granger et al., 2008; Kritee et al., 2012). For example, on the 14th day of the incubation in 2015, NO_3^- concentrations slightly increased in three of the four forest soils (from 0.13 ± 0.02 μg N g^{-1} in the 7th day to 0.65 ± 0.03 μg N g^{-1} in the 14th day, $P < 0.05$), while both ^{15}N and ^{18}O values of NO_3^- decreased by 6.9‰ to 40.6‰ (Fig. S3). Heterotrophic nitrification (not affected by the autotrophic nitrifier inhibitor) may be responsible for the low production of

277 NO_3^-. NO_3^- production may have also occurred in other periods of the incubation. In
278 those cases, the results in the later part of the incubation were excluded from the
279 isotope effect calculation (Figs. 2 to 5).

280 In addition, previous studies of soils determined the N isotope effect during
281 denitrification using the difference between the substrate ($\delta^{15}N_{substrate}$) and product
282 ($\delta^{15}N_{product}$) (Grabb et al., 2017; Lewicka-Szczebak et al., 2014; Lewicka-Szczebak et
283 al., 2015; Mathieu et al., 2007; Menyailo and Hungate, 2006; Perez et al., 2006;
284 Snider et al., 2009; Well and Flessa, 2009). According to Mariotti et al. (1981), when
285 $\delta^{15}N_{substrate}$ is small with regard to 1000, $^{15}\varepsilon$ can be calculated using the following
286 equation:

287 $$^{15}\varepsilon = \delta^{15}N_{substrate} - \delta^{15}N_{product} \quad (3).$$

288 However, when s substantial amount of NO_3^- substrate is consumed, Equation 3
289 does not hold and $^{15}\varepsilon$ can be calculated using the following equation:

290 $$\delta^{15}N_{product} = \delta^{15}N_{substrate} - {}^{15}\varepsilon \, f \ln f / (1-f) \quad (4),$$

291 where $f = [NO_3^-] / [NO_3^-]_{initial}$.

292 To compare our results to those of previous studies, we calculated the N isotope
293 effect of denitrification using the ^{15}N natural abundance of product N_2O. We used the
294 mean $\delta^{15}N$ value of NO_3^- at the beginning of experiment to estimate the $\delta^{15}N$ of the
295 substrate. At the same time, we calculated the N isotope effect using Equation 4 (in 14
296 days) and Equation 3 (in 3 days) using the mean value as $^{15}\varepsilon$.

297 **2.5 Statistical analysis**

298 All analyses were conducted using SPSS software (version 19.0; SPSS Inc., Chicago,
299 IL, U.S.A.). One-way ANOVA was conducted to examine the differences in the
300 investigated soil property variables among forests. Pearson correlation analysis was

performed to examine the correlation between N and O isotopes. Statistically significant differences were set at a P-value of 0.05 unless otherwise stated.

3 Results

3.1 Soil properties

All forest soils examined were acidic, with pH values ranging from 4.1 to 5.3 (Table S2), and the pH of the tropical forest soils (JFL-PF and JFL-SF, averaging 4.1 and 4.2, respectively) was significantly lower than that of the temperate forest soils (QY-LF and QY-MF, averaging 5.1 and 5.3, respectively) ($P < 0.05$). Total C and total N concentrations varied from 1.9% to 4.5% and 0.18% to 0.46%, respectively, and were approximately twice as high in the temperate mixed forest soils as in the other three forest soils. Soil C/N ratios were similar among all four forests (Table S2).

3.2 Nitrate N- and O-isotope fractionation under anaerobic conditions

When forest-level composite soils were incubated under anaerobic conditions, NO_3^- concentrations quickly decreased, and NO_3^- was almost completely consumed within 14 days in all forest soils except the temperate mixed forest soil in 2016 (Fig. 1). The NO_3^- reduction rate ranged from 0.17 to 0.35 μg N g^{-1} h^{-1} (on average 0.26 ± 0.02 μg N g^{-1} h^{-1}) in the first 3 days (in temperate forest soils in 2015 and all tropical forest soils) or 14 days (in temperate mixed forest soils in 2016). Nitrite was not detected or was near the detection limit (0.02 mg L^{-1}) for all forest soils during the entire incubation, while NH_4^+ slightly increased over time in all forest soils (Fig. S4).

With NO_3^- consumption, the $\delta^{18}O$ and $\delta^{15}N$ of the residual NO_3^- increased (Figs. S5 and S6). As predicted by the Rayleigh model, there were significant linear relationships between the $\delta^{18}O$ and $\delta^{15}N$ values against the natural logarithm of the fraction of remaining NO_3^-. The slopes of the lines approximate the N- and O-isotope effect ($^{18}\varepsilon$ and $^{15}\varepsilon$). Nitrogen isotope effects ($^{15}\varepsilon$) spanned a broad range, between

30.8‰ and 65.0‰ (on average 42.3 ± 4.7‰), and $^{18}\varepsilon$ ranged from 10.7‰ to 23.3‰ (on average 15.6 ± 1.1‰) in the studied forest soils (Figs. 2 to 4, Table 1). The slopes of the $\Delta\delta^{18}O$:$\Delta\delta^{15}N$ ratio of the four forest soils had a narrow range, between 0.29 and 0.47, with a mean ratio of 0.34 ± 0.02 (Figs. 2 to 4, Table 1). These variations in $^{15}\varepsilon$ were found to correspond to the incubation conditions, e.g., initial NO_3^- concentrations and DCD (Table 1). An increase in the initial NO_3^- concentrations induced an increase in $^{15}\varepsilon$, from 34.3‰ to 39.5‰ in the tropical primary forest (JFL-PF) soils and from 45.7‰ to 65.0‰ in the temperate mixed forest (QY-MF) soils (Table 1). In addition, with the same initial NO_3^- concentrations, nitrogen isotope effects ($^{15}\varepsilon$) exhibited a greater $^{15}\varepsilon$ when soils were incubated with DCD (Table 1).

In addition, when the plot-level composite soil was incubated with the addition of 20 μg N g^{-1} soil, the NO_3^- reduction rate was on average 0.30 ± 0.02 μg N g^{-1} h^{-1} (in the first 3 days) and 0.22 ± 0.03 μg N g^{-1} h^{-1} (in 14 days) for the tropical primary forest and the temperate mixed forest, respectively, similar to the rates at the forest level (Fig. 1). With decreasing NO_3^- concentration, the $\delta^{18}O$ and $\delta^{15}N$ of the residual NO_3^- also increased (Figs. S5 and S6). The average $^{18}\varepsilon$ was 13.9 ± 0.9‰ and 20.9 ± 0.4‰, and the average $^{15}\varepsilon$ was 41.8 ± 0.4‰ and 54.0 ± 0.4‰ for the tropical primary forest and the temperate mixed forest soils, respectively (Fig. 5, Table 2). The $\Delta\delta^{18}O$:$\Delta\delta^{15}N$ ratios were 0.33 ± 0.2 and 0.39 ± 0.1, respectively (Fig. 5, Table 2).

Under anaerobic conditions, in certain cases, NO_3^- was almost completely consumed after several days (7 days or 14 days), and when the residual NO_3^- amount was less than one-tenth of the initial level, the $\delta^{18}O$ and $\delta^{15}N$ of the residual NO_3^- began to fall below the values expected from a constant $^{18}\varepsilon$ and $^{15}\varepsilon$ (Figs. 2 to 5, S4 and S5).

3.3 Nitrate N- and O-isotope fractionation under aerobic conditions

When forest-level composite soils were incubated under aerobic conditions (headspace filled with air), the NO_3^- reduction rate was on average 0.06 ± 0.00 μg N g^{-1} h^{-1} (in 14 days) for the tropical primary forest and the temperate mixed forest, much lower than under anaerobic conditions (Fig. 1). Nitrite was not detected or was near the detection limit in the two forest soils over the entire incubation, while NH_4^+ slightly increased over time in all forest soils (Fig. S4).

With decreasing NO_3^- concentration, the $\delta^{18}O$ and $\delta^{15}N$ of the residual NO_3^- also increased but in a narrow range compared to that under anaerobic conditions (Figs. S5 and S6). When soils were incubated with DCD, $^{15}\varepsilon$ was 43.7‰ and 58.3‰, and $^{18}\varepsilon$ was 19.8‰ and 39.0‰ for the tropical primary forest and the temperate mixed forest soils, respectively (Fig. 4, Table 1). The $\Delta\delta^{18}O$:$\Delta\delta^{15}N$ ratios were 0.43 and 0.60, respectively (Fig. 4, Table 1). When soils were incubated without DCD, $^{15}\varepsilon$ was 52.7‰ and 64.4‰ and $^{18}\varepsilon$ was 24.8‰ and 38.0‰ for the tropical primary forest and the temperate mixed forest soils, respectively (Fig. 4, Table 1), and the $\Delta\delta^{18}O$:$\Delta\delta^{15}N$ ratios were 0.46 and 0.56, respectively (Fig. 4, Table 1).

3.4 N- and O-isotope effect of denitrification determined by N_2O

The N_2O produced by denitrification was ^{15}N depleted at the beginning of incubation in all forest soils and all treatments, ranging from -21.6‰ to -52.6‰ (Table 3). However, the $\delta^{15}N$ of N_2O increased to -17.9‰ to -6.6‰ on the 14th day (Table 3). According to Equation 3, $^{15}\varepsilon$ for the first 3 days ranged from 21.0‰ to 50.4‰ (on average 38.5 ± 8.9‰) and from 55.5‰ to 66.6‰ (on average 60.7 ± 3.2‰) for the tropical primary forest soils and temperate mixed forest soils, respectively. In addition, $^{15}\varepsilon$ for the entire 14-day incubation was calculated using Equation 4, ranging from 38.4‰ to 77.4‰ (on average 60.0 ± 11.4‰) and 65.1‰ to 74.0‰ (on average 70.0 ± 2.6‰) for the primary forest soils and mixed forest soils, respectively.

4 Discussion

4.1 N isotope fractionation during denitrification

Our study shows that the apparent N isotope effect ($^{15}\varepsilon$) during denitrification under strictly anaerobic conditions and at room temperature for soils from the four study forests ranged from 30.8‰ to 65.0‰ (on average 48.3 ± 2.0‰, Tables 1 and 2). Our results are, unexpectedly, largely outside of the reported range of previous studies (Fig. 6); for example, values of 6‰ to 33‰ were reported for temperate agricultural soil (Blackmer and Bremner, 1977; Chien et al., 1977; Mariotti et al., 1982); 13‰ for the field incubation of Hawaiian tropical forest soils (Houlton et al., 2006); 10‰ to 45‰ for three tropical forests in the Brazilian Amazon (Perez et al., 2006); 20‰ to 29‰ for two temperate forests in central Ontario, Canada (Snider et al., 2009); and 24‰ to 29‰ for two boreal forests in Krasnoyarsk, Russia (Menyailo and Hungate, 2006). Our values are also higher than the $^{15}\varepsilon$ reported for many other environments, e.g., 5‰ to 30‰ in pure culture studies of heterotrophic denitrifying bacteria (Granger et al., 2008; Treibergs and Granger, 2016 , and references therein) and 18‰ for permeable sediments (Kessler et al., 2014). We also determined the N_2O produced during the 2016 incubation and found that the $^{15}\varepsilon$ of NO_3^- to N_2O calculated by $\delta^{15}N\text{-}NO_3^-$ and $\delta^{15}N\text{-}N_2O$ was, on average, 49‰ and 65‰, respectively (Table 3). These results were also at the upper limit of other soil studies determined via the same approach for agricultural soils (2‰ to 55‰) (Grabb et al., 2017; Lewicka-Szczebak et al., 2014; Lewicka-Szczebak et al., 2015; Mathieu et al., 2007; Well and Flessa, 2009) and forest soils (10‰ to 45‰) (Menyailo and Hungate, 2006; Perez et al., 2006; Snider et al., 2009).

Although N isotope enrichment factors ($^{15}\varepsilon$) observed in the present study were higher than previously observed, the range of values we observed (31‰ to 65‰,

401 Tables 1 and 2) was nevertheless within that predicted by theory. According to the
402 efflux model proposed by Kohl and Shearer (1978), the $^{15}\varepsilon_{organism}$ (at the organism
403 level), as measured in our study, integrates the isotope effect that occurs during the
404 uptake step from the medium to the cell through the cell membrane ($^{15}\varepsilon_{uptake}$) and the
405 isotope effect that occurs during NO_3^- reduction within the cell ($^{15}\varepsilon_{intrinic}$). The uptake
406 step will present a low isotopic fractionation. For a case of simple diffusion, this
407 fractionation depends on the square root of the mass ratio of the two isotopic species;
408 in this case, $^{15}NO_3^-$ and $^{14}NO_3^-$ for N isotope effect (resulting in a $^{15}\varepsilon_{uptake}$ of 8‰). The
409 NO_3^- reduction step is the rate-limiting and irreversible step that involves enzymatic
410 breakage of the N-O bond, which results in a large isotope fractionation of 65.9‰ at
411 25 °C (Urey, 1947). Thus, the maximum $^{15}\varepsilon_{organism}$ will be approximately 74‰, higher
412 than the highest record in our study of forest soils.

413 The initial NO_3^- concentration has been shown to affect the isotope effect of
414 denitrification (Mariotti et al., 1982). When the initial NO_3^- concentration is low, NO_3^-
415 reduction is relatively more complete and NO_3^- uptake is the rate-limiting step, which
416 may cause a negligible isotope fractionation (Granger et al., 2004; Granger et al.,
417 2008). In this case, $^{15}\varepsilon$ was low due to the low efflux/uptake ratio (Wenk et al., 2014).
418 However, with increased initial NO_3^- concentration, NO_3^- reductase was no longer
419 sufficient to sustain maximal reduction rates (i.e., the enzymatic step became the
420 rate-limiting step), and the intrinsic isotope fractionation could be nearly fully
421 expressed in the environment (i.e., higher $^{15}\varepsilon$) (Mariotti et al., 1982; Wenk et al.,
422 2014). Our results were consistent with this interpretation. We found that initial NO_3^-
423 concentration was positively correlated with $^{15}\varepsilon$, i.e., a higher initial NO_3^-
424 concentration was associated with a higher fractionation (Table 1). The treatments
425 with 20 μg NO_3^--N g^{-1} soil had a higher $^{15}\varepsilon$ (39.5‰ and 65.0‰ for the tropical

primary forest and the temperate mixed forest soils, respectively) than treatments with 10 μg NO_3^--N g^{-1} soil ($^{15}\varepsilon$ was 34.3‰ and 52.7‰, respectively) and those without N addition ($^{15}\varepsilon$ was 45.7‰ for temperate mixed forest).

Previous studies also showed that $^{15}\varepsilon$ was affected by temperature and the amount of available organic carbon (Maggi and Riley, 2015; Mariotti et al., 1982; Wunderlich et al., 2012). These effects primarily arise because denitrification rates are regulated by temperature and the quantity of electron donors. Mariotti et al. (1982) reported that $^{15}\varepsilon$ was highly correlated with denitrification rate for the studied agricultural soil, with $^{15}\varepsilon$ exponentially decreasing with an increasing denitrification rate (expressed as rate constant k_1) (Mariotti et al., 1988). Similar to this finding, across all forest soils in the present study, $^{15}\varepsilon$ was also found to exponentially decrease with increasing denitrification rate (Fig. 7). However, our results were still greater than the values observed in agricultural soil incubation with the same denitrification rate (Blackmer and Bremner, 1977; Chien et al., 1977; Mariotti et al., 1982).

In addition, the denitrifying bacterial communities and/or availability of nutrients and dissolved organic matter impacted by $^{15}\varepsilon$ may differ across soil types. Different forest soils may have distinct denitrifying bacterial communities, or if the bacterial communities are similar, they may have a different isotopic effect due to differential enzymatic isotope expression. Studies have shown that denitrifying communities were related to soil C/N ratios (Rich et al., 2003) and vegetation types (Menyailo, 2007). For example, the $^{15}\varepsilon$ in the tropical primary forest was always lower than that in the temperate mixed forest even when they received the same nutrient and temperature treatments (Table 1). Additionally, we found that $^{15}\varepsilon$ (51.4‰) for the temperate mixed forest soils in 2015 was lower than that in 2016 (65.0‰), which had a different initial NO_3^- concentration and denitrification rate (Table 1, Fig. 1). This finding may provide

451 further evidence that the N isotope effect of denitrification was correlated with the
452 initial NO_3^- concentration and denitrification rate (Mariotti et al., 1982).

453 It remains unclear why $^{15}\varepsilon$ was higher for our study forests than for the other
454 forest soils reported in previous studies. We propose two potential mechanisms. First,
455 the method using ^{15}N depletion of N_2O relative to NO_3^- may underestimate $^{15}\varepsilon$
456 because N_2O is likely to be further reduced to N_2, such that the remaining N_2O
457 becomes more ^{15}N enriched than it should be, although this was not the case in the
458 forest soils in the present study, where 25% to 60% of produced N_2O was shown to be
459 further reduced to N_2 under anaerobic conditions (Xi, 2016). This method has been
460 used in three of the four previous studies for forest soils to determine $^{15}\varepsilon$ during
461 denitrification (Menyailo and Hungate, 2006; Perez et al., 2006; Snider et al., 2009).
462 Second, relatively complete NO_3^- reduction may explain the low $^{15}\varepsilon$ observed in the
463 first 10 cm mineral soil in Hawaiian tropical forests, which results in an
464 underexpression of N isotope effects (Houlton et al., 2006). Partial NO_3^- consumption
465 (‘‘open-system kinetics’’) leaves behind ^{15}N-enriched NO_3^-, which can diffuse out of
466 the zone of ongoing denitrification, while complete NO_3^- consumption
467 (‘‘closed-system kinetics’’) would cause underexpression of the isotope effect because
468 little or no ^{15}N-rich NO_3^- would escape. In fact, denitrification in the soil below a
469 depth of 10 cm should exhibit a high N isotope effect (60‰, comparable to our results)
470 across the Hawaiian tropical forests; therefore, the relationship between $^{15}N/^{14}N$ of
471 NO_3^- and $\ln([NO_3^-])$ in the profile can be appropriately fitted (Houlton, 2005).

472 **4.2 Oxygen isotope fractionation and $\Delta\delta^{18}O$:$\Delta\delta^{15}N$ ratio in NO_3^- during**
473 **denitrification**

474 Unlike the large N-isotope effect, the O-isotope effect ($^{18}\varepsilon$) in our forest soils was
475 small. The mean value of $^{18}\varepsilon$ was 16.2 ± 0.9‰, comparable to other studies, e.g., 5‰

to 24‰ in the pure culture studies of heterotrophic denitrifying bacteria (Dabundo, 2014; Frey et al., 2014; Granger et al., 2008; Hosono et al., 2015; Karsh et al., 2012; Knöeller et al., 2011; Kritee et al., 2012; Treibergs and Granger, 2016; Wunderlich et al., 2012), 14.2‰ in permeable sediments (Kessler et al., 2014), and 7‰ to 18‰ in groundwater (Böttcher et al., 1990; Fukada et al., 2003; Mengis et al., 1999; Wenk et al., 2014). As in the $\delta^{15}N$ of the residual NO_3^-, $\delta^{18}O$ also began to fall below the values expected from a constant $^{18}\varepsilon$ when the residual NO_3^- amount was less than one-tenth of the initial value (Figs. 2 to 5).

Due to the relatively higher $^{15}\varepsilon$, the ratio of $\Delta\delta^{18}O$:$\Delta\delta^{15}N$ was lower, at 0.34 ± 0.01 across all forest soils. This ratio is significantly lower than the ratio of 1 for denitrification bacteria (which is expected because of the stronger ^{15}N effect but similar ^{18}O effect). The ratios in the present study are also lower relative to the reported range for terrestrial environments (0.47 to 0.89) (Böttcher et al., 1990; Fukada et al., 2003; Lehmann et al., 2003; Wenk et al., 2014), marine environments (1.25) (Sigman et al., 2005) and the pure culture of heterotrophic denitrifying bacteria (0.33 to 1.02) (Dabundo, 2014; Frey et al., 2014; Granger et al., 2008; Hosono et al., 2015; Karsh et al., 2012; Knöeller et al., 2011; Kritee et al., 2012; Treibergs and Granger, 2016; Wunderlich et al., 2012). In addition, our result was lower than the ratio of $\Delta\delta^{18}O$: $\Delta\delta^{15}N$ in soil water and stream water from tropical forest studies (1.11-1.54 and 0.66, respectively) (Fang et al., 2015; Houlton et al., 2006), but similar to the value for a temperate forest (0.30) (Fang et al., 2015).

One possible explanation for the lower ratio of $\Delta\delta^{18}O$:$\Delta\delta^{15}N$ may be related to the different fractionation of N and O isotopes via internal enzymatic reduction. During denitrification, there are two types of dissimilatory NO_3^- reductases: bacterial membrane-bound NO_3^- reductase (Nar) and periplasmic NO_3^- reductase (Nap).

Evidence suggested that the differences in the catalytic steps between Nar and Nap would be responsible for the lower ratio of $\Delta\delta^{18}O$:$\Delta\delta^{15}N$ under anaerobic conditions (Frey et al., 2014; Wenk et al., 2014). Nap can split not only light O but also heavy O, leading to a slower enrichment of ^{18}O than of ^{15}N in NO_3^- (Frey et al., 2014); thus, Nap enzymes may be responsible for the relatively low $\Delta\delta^{18}O$:$\Delta\delta^{15}N$ ratio. Previous studies of a pure culture of heterotrophic denitrifying bacteria and in Lake Lugano were consistent with this finding (Frey et al., 2014; Granger et al., 2008; Treibergs and Granger, 2016; Wenk et al., 2014). Moreover, under NO_3^--limited conditions, Nap can be essential for NO_3^- reduction due to its higher affinity for NO_3^-, and the relative abundance of NapA genes has been shown to increase with decreasing NO_3^- concentrations (Dong et al., 2009).

Another potential explanation for the lower $\Delta\delta^{18}O$:$\Delta\delta^{15}N$ ratio is the O isotope exchange between NO_2^- and water and the production of NO_3^- via NO_2^- oxidation (NXR) through anaerobic ammonium oxidation (anammox) (Granger and Wankel, 2016). Granger and Wankel (2016) recently proposed a numerical model of NO_3^- isotope dynamics and suggested that when the NXR/NAR ratio was low (i.e. NO_2^- was mostly reduced to NO rather than oxidized to NO_3^-), the $\delta^{15}N$ of NO_2^- was relatively more ^{15}N enriched and the NO_3^- produced by NO_2^- oxidation was further ^{15}N enriched due to the inverse isotope effect (Casciotti, 2009). In contrast, the $\delta^{18}O$ of NO_3^- produced by NO_2^- oxidation would decrease due to the O-isotope exchange between NO_2^- and water and the incorporation of O from water into NO_3^- (Fang et al., 2012; Kool et al., 2009; Wunderlich et al., 2013). The anammox process will increase $\delta^{15}N$ of residual NO_3^- and lower the $\Delta\delta^{18}O$:$\Delta\delta^{15}N$ ratio. Wunderlich et al. (2013) also found that a redox NO_2^- and NO_3^- cycle driven by nitrite oxidoreductase (Nxr) may occur under moderate pH and anaerobic conditions, resulting in modification of the

526 $\Delta\delta^{18}O:\Delta\delta^{15}N$ ratio during denitrification. Moreover, O-isotope exchange is regulated
527 by pH, with higher rates of isotope exchange at lower pH values (Kaneko and Poulson,
528 2013). In our study, soil pH, which ranged from 4.1 to 5.3, was positively correlated
529 with $^{18}\varepsilon$ ($R^2 = 0.83$, $P < 0.05$, Fig. S7), which suggests that pH may affect the extent of
530 O-isotope exchange and the $\Delta\delta^{18}O:\Delta\delta^{15}N$ ratio.

531 **4.3 Implications for estimating denitrification rates**

532 Our study revealed an unexpectedly high N isotope effect during denitrification, with
533 an average value of 48‰ across all experiments. In previous ecosystem studies that
534 used a $^{15}\varepsilon$ of 16‰ to estimate the effects of denitrification on isotopes, the
535 denitrification was estimated to account for 35% of total N losses from global
536 unmanaged terrestrial ecosystems and for 48% to 86% for the six studied forests in
537 southern China and central Japan (Fang et al., 2015; Houlton and Bai, 2009).
538 However, if we instead apply our averaged value of 48‰ during denitrification, we
539 find that the proportion of denitrification in total N losses would decrease to 12% for
540 the Houlton and Bai (2009) study and to 26% to 68% for the Fang et al. (2015) study.
541 Our new estimates indicate that the contribution of denitrification to N losses might
542 have been considerably overestimated for soils bearing a high N isotope fractionation
543 in previous studies. However, the extent to which these findings are representative of
544 ecosystems at a larger scale is uncertain due to soil spatial heterogeneity. Therefore, it
545 will be important to confirm whether this observed high N isotope fractionation is
546 indeed typical for forest ecosystems worldwide.

547 **5 Conclusion**

548 In this study, soils from two tropical and two temperate forests in China were
549 incubated under both anaerobic and aerobic conditions to determine the isotope
550 fractionation of N and O of NO_3^- during denitrification as well as the ratio of

551 $\Delta\delta^{18}O$:$\Delta\delta^{15}N$. We found that the N isotope effects were, unexpectedly, much higher
552 than the reported range of heterotrophic denitrification and other environmental
553 settings (e.g., groundwater, marine sediments and agricultural soils), ranging from
554 31‰ and 65‰ in the studied forest soils. These variations in $^{15}\varepsilon$ were found to
555 correspond to the incubation conditions, e.g., initial NO_3^- concentrations and DCD.
556 However, the O-isotope effect ($^{18}\varepsilon$) of our forest soils was comparable to that in other
557 studies, ranging from 11‰ to 39‰. In addition, the ratios of $\Delta\delta^{18}O$:$\Delta\delta^{15}N$ ranged
558 from 0.28 to 0.60, which were lower than the canonical ratios of 0.5 to 1 for
559 denitrification bacteria and other terrestrial environments. We suggest that the isotope
560 effect of denitrification for soils may vary greatly with region and soil type.
561 Furthermore, our new estimates for denitrification rates indicate that the contribution
562 of denitrification to N loss might have been considerably overestimated for soils in
563 previous studies in which lower fractionation factors were used.

Appendix A

Contents of this file:

Table S1 - Table S3

Figure S1 - Figure S7

Acknowledgements: This work was financially supported by the National Key Research and Development Program of China (grant number 2016YFA0600802); the Strategic Priority Research Program of Chinese Academy of Sciences (grant number XDB15020200); the National Natural Science Foundation of China (grant numbers 31370464, 31422009 and 41773094); the Key Research Program of Frontier Sciences, CAS, and the Hundred Talents Program of Chinese Academy of Sciences (grant number Y1SRC111J6). The work was also jointly supported by the Jianfengling National Key Field Station. We are grateful to Dr. Sarah A. Batterman for suggestions for the organization of the manuscript, the presentation of results and the novelty of the study as well as numerous edits of the language. Constructive comments by reviewers and the editor have greatly improved the quality of this paper. The authors declare no competing financial interests.

References

Aravena, R., Robertson, W.D., 1998. Use of multiple isotope tracers to evaluate denitrification in ground water: Study of nitrate from a large-flux septic system plume. Ground Water 36, 975-982. DOI: 10.1111/j.1745-6584.1998.tb02104.x

Böttcher, J., Strebel, O., Voerkelius, S., Schmidt, H.L., 1990. Using isotope fractionation of nitrate nitrogen and nitrate oxygen for evaluation of microbial denitrification in a sandy aquifer. J. Hydrol. 114, 413-424. DOI: 10.1016/0022-1694(90)90068-9

Barford, C.C., Montoya, J.P., Altabet, M.A., Mitchell, R., 1999. Steady-state nitrogen isotope effects of N_2 and N_2O production in Paracoccus denitrificans. Appl. Environ. Microbiol. 65, 989-994.

Blackmer, A.M., Bremner, J.M., 1977. Nitrogen isotope discrimination in denitrification of nitrate in soils. Soil Biol. Biochem. 9, 73-77. DOI: 10.1016/0038-0717(77)90040-2

Brandes, J.A., Devol, A.H., 1997. Isotopic fractionation of oxygen and nitrogen in coastal marine sediments. Geochim. Cosmochim. Acta 61, 1793-1801. DOI: 10.1016/s0016-7037(97)00041-0

Brandes, J.A., Devol, A.H., 2002. A global marine-fixed nitrogen isotopic budget: Implications for Holocene nitrogen cycling. Global Biogeochem. Cycles 16. DOI: 10.1029/2001gb001856

Brandes, J.A., Devol, A.H., Yoshinari, T., Jayakumar, D.A., Naqvi, S.W.A., 1998. Isotopic composition of nitrate in the central Arabian Sea and eastern tropical North Pacific: A tracer for mixing and nitrogen cycles. Limnol. Oceanogr. 43, 1680-1689. DOI: 10.4319/lo.1998.43.7.1680

605 Buffen, A.M., Hastings, M.G., Thompson, L.G., Mosley-Thompson, E., 2014.
606 Investigating the preservation of nitrate isotopic composition in a tropical ice
607 core from the Quelccaya Ice Cap, Peru. J. Geophys. Res.: Atmospheres 119,
608 2674-2697. DOI:10.1002/2013jd020715
609 Casciotti, K.L., 2009. Inverse kinetic isotope fractionation during bacterial nitrite
610 oxidation. Geochim. Cosmochim. Acta. 73, 2061-2076.
611 DOI:http://dx.DOI.org/10.1016/j.gca.2008.12.022
612 Chen, D., Li, Y., Liu, H., Xu, H., Xiao, W., Luo, T., Zhou Z., Lin M.X., 2010.
613 Biomass and carbon dynamics of a tropical mountain rain forest in China. Sci.
614 China-life. Sci. 53, 798-810. DOI: 10.1007/s11427-010-4024-2
615 Chien, S.H., Shearer, G., Kohl, D.H., 1977. The nitrogen isotope effect associated with
616 nitrate and nitrite loss from waterlogged soils. Soil Sci. Soc. Am. J. 41, 63-69.
617 DOI: 10.2136/sssaj1977.03615995004100010021x
618 Cline, J.D., Kaplan, I.R., 1975. Isotopic fractionation of dissolved nitrate during
619 denitrification in the eastern tropical north pacific ocean. Mar. Chem. 3,
620 271-299. DOI:10.1016/0304-4203(75)90009-2
621 Dähnke, K., Thamdrup, B., 2015. Isotope fractionation and isotope decoupling during
622 anammox and denitrification in marine sediments. Limnol. Oceanogr. 61,
623 610-624. DOI: 10.1002/lno.10237
624 Dabundo, R., 2014. Nitrogen isotopes in the measurement of N_2-fixation and the
625 estimation of denitrification in the global ocean. Master's Theses 703.
626 Delwiche, C.C., Steyn, P.L., 1970. Nitrogen isotope fractionation in soils and
627 microbial reactions. Environ. Sci. Technol. 4, 929-935. DOI:
628 10.1021/es60046a004
629 Dong, L.F., Smith, C.J., Papaspyrou, S., Stott, A., Osborn, A.M., Nedwell, D.B., 2009.

630 Changes in benthic denitrification, nitrate ammonification, and anammox
631 process rates and nitrate and nitrite reductase gene abundances along an
632 estuarine nutrient gradient (the colne estuary, united kingdom). Appl. Environ.
633 Microbiol. 75, 3171-3179. DOI: 10.1128/aem.02511-08
634 Fang, J., Li, Y., Zhu, B., Liu, G., Zhou, G., 2004. Community structures and species
635 richness in the montane rain forest of Jianfengling, Hainan Island, China.
636 Biodivers. Sci. 12, 29-43.
637 Fang Y.T., Koba K., Makabe A., Takahashi C., Zhu W.X., Hayashi T., Hokari A.,
638 Urakawa R., Bai E., Houlton B.Z., Xi D., Zhang S.S., Matsushita K., Tu Y.,
639 Liu D.W., Zhu F.F., Wang Z., Zhou G., Chen D., Makita T., Toda H., Liu X.,
640 Chen Q., Zhang D., Li Y., Yoh M., 2015. Microbial denitrification dominates
641 nitrate losses from forest ecosystems. Proc. Natl. Acad. Sci. U. S. A. 112,
642 1470-1474. DOI: 10.1073/pnas.1416776112
643 Fang, Y.T., Koba, K., Makabe, A., Zhu, F.F., Fan, S.Y., Liu, X.Y., Yoh M., 2012. Low
644 delta O-18 Values of Nitrate Produced from Nitrification in Temperate Forest
645 Soils. Environ. Sci. Technol. 46, 8723-8730. DOI: 10.1021/es300510r
646 Frey, C., Hietanen, S., Jurgens, K., Labrenz, M., Voss, M., 2014. N and O isotope
647 fractionation in nitrate during chemolithoautotrophic denitrification by
648 Sulfurimonas gotlandica. Environ. Sci. Technol. 48, 13229-13237. DOI:
649 10.1021/es503456g
650 Fukada, T., Hiscock, K.M., Dennis, P.F., Grischek, T., 2003. A dual isotope approach
651 to identify denitrification in groundwater at a river-bank infiltration site. Water
652 Res. 37, 3070-3078. DOI: 10.1016/s0043-1354(03)00176-3
653 Grabb, K.C., Buchwald, C., Hansel, C.M., Wankel, S.D., 2017. A dual nitrite isotopic
654 investigation of chemodenitrification by mineral-associated Fe(II) and its

655 production of nitrous oxide. Geochim. Cosmochim. Acta 196, 388-402.
656 DOI:10.1016/j.gca.2016.10.026
657 Granger, J., Sigman, D.M., Lehmann, M.F., Tortell, P.D., 2008. Nitrogen and oxygen
658 isotope fractionation during dissimilatory nitrate reduction by denitrifying
659 bacteria. Limnol. Oceanogr. 53, 2533-2545. DOI: 10.4319/lo.2008.53.6.2533
660 Granger, J., Wankel, S.D., 2016. Isotopic overprinting of nitrification on
661 denitrification as a ubiquitous and unifying feature of environmental nitrogen
662 cycling. Proc. Natl. Acad. Sci. U. S. A. 113, E6391-E6400. DOI:
663 10.1073/pnas.1601383113
664 Groffman, P.M., Altabet, M.A., Böhlke, J., Butterbach-Bahl, K., David, M.B.,
665 Firestone, M.K., Giblin A.E., Kana T.M., Nielsen L.P., Voytek M.A. 2006.
666 Methods for measuring denitrification: diverse approaches to a difficult
667 problem. Ecol. Appl. 16, 2091-2122. DOI:
668 10.1890/1051-0761(2006)016[2091:MFMDDA]2.0.CO;2
669 Gruber, N., Galloway, J.N., 2008. An Earth-system perspective of the global nitrogen
670 cycle. Nature 451, 293-296. DOI: 10.1038/nature06592
671 Harris, E., Emmenegger, L., Mohn, J., 2017. Using isotopic fingerprints to trace
672 nitrous oxide in the atmosphere. CHIMIA International Journal for Chemistry
673 71, 46-46.
674 Hosono, T., Alvarez, K., Lin, I.T., Shimada, J., 2015. Nitrogen, carbon, and sulfur
675 isotopic change during heterotrophic (Pseudomonas aureofaciens) and
676 autotrophic (Thiobacillus denitrificans) denitrification reactions. J. Contam.
677 Hydrol. 183, 72-81. DOI: 10.1016/j.jconhyd.2015.10.009
678 Houlton, B.Z., 2005. Isotopic evidence for the climate dependence of itrogen cycles
679 across old tropical rainforests, Mt. Haleakala, Hawaii. Doctoral dissertation.

680 Houlton, B.Z., Bai, E., 2009. Imprint of denitrifying bacteria on the global terrestrial
681 biosphere. Proc. Natl. Acad. Sci. U. S. A. 106, 21713-21716. DOI:
682 10.1073/pnas.0912111106
683 Houlton, B.Z., Sigman, D.M., Hedin, L.O., 2006. Isotopic evidence for large gaseous
684 nitrogen losses from tropical rainforests. Proc. Natl. Acad. Sci. U. S. A. 103,
685 8745-8750. Doi:10.1073/pnas.0510185103
686 Kaneko, M., Poulson, S.R., 2013. The rate of oxygen isotope exchange between
687 nitrate and water. Geochim. Cosmochim. Acta 118, 148-156. DOI:
688 10.1016/j.gca.2013.05.010
689 Karsh, K.L., Granger, J., Kritee, K., Sigman, D.M., 2012. Eukaryotic assimilatory
690 nitrate reductase fractionates N and O isotopes with a ratio near unity. Environ.
691 Sci. Technol. 46, 5727-35. DOI:10.1021/es204593q
692 Kendall, C., Elliott, E.M., Wankel, S.D., 2007. Tracing anthropogenic inputs of
693 nitrogen to ecosystems. In Stable Isotopes in Ecology and Environmental
694 Science R.H. Michener and K. Lajtha Eds.; Blackwell Publishing: 2007, pp
695 375-449.
696 Kessler, A.J., Bristow, L.A., Cardenas, M.B., Glud, R.N., Thamdrup, B., Cook, P.L.M.,
697 2014. The isotope effect of denitrification in permeable sediments. Geochim.
698 Cosmochim. Acta 133, 156-167. DOI: 10.1016/j.gca.2014.02.029
699 Kim, K.R., Craig, H., 1990. Two-isotope characterization of N_2O in the Pacific Ocean
700 and constraints on its origin in deep water. Nature 347, 58-61.
701 DOI:10.1038/347058a0
702 Knöeller, K., Vogt, C., Haupt, M., Feisthauer, S., Richnow, H.H., 2011. Experimental
703 investigation of nitrogen and oxygen isotope fractionation in nitrate and nitrite
704 during denitrification. Biogeochemistry 103, 371-384. DOI:

705 10.1007/s10533-010-9483-9
706 Kohl, D., Shearer, G. Isotope effects in metabolic studies. Recent Developments in
707 Mass Spectrometry in Biochemistry and Medicine. Springer, 1978, pp.
708 623-640.
709 Kool, D.M., Müller, C., Wrage, N., Oenema, O., Van Groenigen, J.W., 2009. Oxygen
710 exchange between nitrogen oxides and H_2O can occur during nitrifier
711 pathways. Soil Biol. Biochem. 41, 1632-1641.
712 DOI:10.1016/j.soilbio.2009.05.002
713 Kritee, K., Sigman, D.M., Granger, J., Ward, B.B., Jayakumar, A., Deutsch, C., 2012.
714 Reduced isotope fractionation by denitrification under conditions relevant to
715 the ocean. Geochim. Cosmochim. Acta 92, 243-259. DOI:
716 10.1016/j.gca.2012.05.020
717 Lehmann, M.F., Reichert, P., Bernasconi, S.M., Barbieri, A., McKenzie, J.A., 2003.
718 Modelling nitrogen and oxygen isotope fractionation during denitrification in a
719 lacustrine redox-transition zone. Geochim. Cosmochim. Acta 67, 2529-2542.
720 DOI: 10.1016/s0016-7037(03)00085-1
721 Lewicka-Szczebak, D., Well, R., Köster, J.R., Fuß, R., Senbayram, M., Dittert, K., et
722 al., 2014. Experimental determinations of isotopic fractionation factors
723 associated with N_2O production and reduction during denitrification in soils.
724 Geochim. Cosmochim. Acta 134, 55-73. DOI:10.1016/j.gca.2014.03.010
725 Lewicka-Szczebak, D., Well, R., Bol, R., Gregory, A.S., Matthews, G.P., Misselbrook,
726 T., Whalley W.R., Cardenas L.M., 2015. Isotope fractionation factors
727 controlling isotopocule signatures of soil-emitted N_2O produced by
728 denitrification processes of various rates. Rapid Commun. Mass Spectrom. 29,
729 269-282. DOI: 10.1002/rcm.7102

730 Luo, T., Li, Y., Chen, D., Lin, M., Sun, Y., 2005. A study on the soil properties of
731 dacrycarpus imbricatus Bl. plantation in tropical mountainous region in
732 Hainan Island. Natural Sci J of Hainan University 23, 340-346.
733 Maggi, F., Riley, W.J., 2015. The effect of temperature on the rate, affinity, and 15N
734 fractionation of NO_3^- during biological denitrification in soils.
735 Biogeochemistry 124, 235-253. DOI:10.1007/s10533-015-0095-2
736 Mariotti, A., Germon, J., Hubert, P., Kaiser, P., Letolle, R., Tardieux, A., Tardieux P.,
737 1981. Experimental determination of nitrogen kinetic isotope fractionation:
738 some principles: illustration for the denitrification and nitrification processes.
739 Plant soil 62, 413-430.
740 Mariotti, A., Germon, J., Leclerc, A., 1982. Nitrogen isotope fractionation associated
741 with the $NO_2^- \rightarrow N_2O$ step of denitrification in soils. Can. J. Soil Sci. 62,
742 227-241. DOI:org/10.4141/cjss82-027
743 Mariotti, A., Landreau, A., Simon, B., 1988. ^{15}N isotope biogeochemistry and natural
744 denitrification process in groundwater: application to the chalk aquifer of
745 northern France. Geochim. Cosmochim. Acta 52, 1869-1878.
746 DOI:org/10.1016/0016-7037(88)90010-5
747 Mathieu, O., Leveque, J., Henault, C., Ambus, P., Milloux, M.J., Andreux, F., 2007.
748 Influence of ^{15}N enrichment on the net isotopic fractionation factor during the
749 reduction of nitrate to nitrous oxide in soil. Rapid Commun. Mass Spectrom.
750 21, 1447-1451. DOI:10.1002/rcm.2979
751 Mengis, M., Schiff, S.L., Harris, M., English, M.C., Aravena, R., Elgood, R.J.,
752 MacLean, A., 1999. Multiple geochemical and isotopic approaches for
753 assessing ground water NO_3^- elimination in a riparian zone. Ground Water 37,
754 448-457. DOI: 10.1111/j.1745-6584.1999.tb01124.x

Menyailo, O.V., 2007. The influence of tree species on the biomass of denitrifying bacteria in gray forest soils. Eurasian Soil Sci. 40, 302-307. DOI: 10.1134/s1064229307030088

Menyailo, O.V., Hungate, B.A., 2006. Stable isotope discrimination during soil denitrification: Production and consumption of nitrous oxide. Global Biogeochem. Cycles 20, n/a-n/a. DOI:10.1029/2005gb002527

Perez, T., Garcia-Montiel, D., Trumbore, S., Tyler, S., Camargo, P.d., Moreira, M., Piccolo M., Cerri C., 2006. Nitrous oxide nitrification and denitrification ^{15}N enrichment factors from Amazon forest soils. Ecol. Appl. 16, 2153-2167. DOI: 10.1890/1051-0761(2006)016[2153:NONADN]2.0.CO;2

Rich, J.J., Heichen, R.S., Bottomley, P.J., Cromack, K., Myrold, D.D., 2003. Community composition and functioning of denitrifying bacteria from adjacent meadow and forest soils. Appl. Environ. Microbiol. 69, 5974-5982. DOI: 10.1128/aem.69.10.5974-5982.2003

Sigman, D.M., Granger, J., DiFiore, P.J., Lehmann, M.M., Ho, R., Cane, G., van Geen A., 2005. Coupled nitrogen and oxygen isotope measurements of nitrate along the eastern North Pacific margin. Global Biogeochem. Cycles 19. DOI: 10.1029/2005gb002458

Sigman, D.M., Robinson, R., Knapp, A.N., van Geen, A., McCorkle, D.C., Brandes, J.A., Thunell R.C., 2003. Distinguishing between water column and sedimentary denitrification in the Santa Barbara Basin using the stable isotopes of nitrate. Geochem. Geophy. Geosy. 4. DOI:10.1029/2002gc000384

Smith, R.L., Howes, B.L., Duff, J.H., 1991. Denitrification in nitrate-contaminated groundwater: Occurrence in steep vertical geochemical gradients. Geochim. Cosmochim. Acta 55, 1815-1825. DOI:org/10.1016/0016-7037(91)90026-2

780 Snider, D.M., Schiff, S.L., Spoelstra, J., 2009. $^{15}N/^{14}N$ and $^{18}O/^{16}O$ stable isotope
781 ratios of nitrous oxide produced during denitrification in temperate forest soils.
782 Geochim. Cosmochim. Acta 73, 877-888. DOI:10.1016/j.gca.2008.11.004
783 Talbot, J.M., Bruns, T.D., Taylor, J.W., Smith, D.P., Branco, S., Glassman, S.I.,
784 Erlandson S., Vilgalys R., Liao H.L., Smith M.E., Peay K.G., 2014. Endemism
785 and functional convergence across the North American soil mycobiome. Proc.
786 Natl. Acad. Sci. U. S. A. 111, 6341-6. DOI:10.1073/pnas.1402584111
787 Treibergs, L.A., Granger, J., 2016. Enzyme level N and O isotope effects of
788 assimilatory and dissimilatory nitrate reduction. Limnol. Oceanogr.
789 DOI:10.1002/lno.10393
790 Tu, Y., Fang, Y., Liu, D., Pan, Y., 2016. Modifications to the azide method for nitrate
791 isotope analysis. Rapid Commun. Mass Spectrom. 30, 1213-1222. DOI:
792 10.1002/rcm.7551
793 Urey, H.C., 1947. The Thermodynumic Properties of Isotopic Substances. J. Chem.
794 Soc., 562-581.
795 Vitousek, P.M., Howarth, R.W., 1991. Nitrogen limitation on land and in the sea: how
796 can it occur? Biogeochemistry 13, 87-115.
797 Vogel, J.C., Talma, A.S., Heaton, T.H.E., 1981. Gaseous nitrogen as evidence for
798 denitrification in groundwater. J. Hydrol. 50, 191-200.
799 DOI:org/10.1016/0022-1694(81)90069-X
800 Voss, M., Dippner, J.W., Montoya, J.P., 2001. Nitrogen isotope patterns in the
801 oxygen-deficient waters of the Eastern Tropical North Pacific Ocean. Deep
802 Sea Res., Part I 48, 1905-1921. DOI: 10.1016/s0967-0637(00)00110-2
803 Well, R., Flessa, H., 2009. Isotopologue signatures of N_2O produced by denitrification
804 in soils. J. Geophy. Res.: Biogeosciences 114, n/a-n/a.

DOI:10.1029/2008jg000804

Wenk, C.B., Zopfi, J., Blees, J., Veronesi, M., Niemann, H., Lehmann, M.F., 2014. Community N and O isotope fractionation by sulfide-dependent denitrification and anammox in a stratified lacustrine water column. Geochim. Cosmochim. Acta 125, 551-563. DOI:10.1029/2008jg000804 DOI:10.1016/j.gca.2013.10.034

Wunderlich, A., Meckenstock, R., Einsiedl, F., 2012. Effect of different carbon substrates on nitrate stable isotope fractionation during microbial denitrification. Environ. Sci. Technol. 46, 4861-4868. DOI: 10.1021/es204075b

Wunderlich, A., Meckenstock, R.U., Einsiedl, F., 2013. A mixture of nitrite-oxidizing and denitrifying microorganisms affects the $\delta^{18}O$ of dissolved nitrate during anaerobic microbial denitrification depending on the $\delta^{18}O$ of ambient water. Geochim. Cosmochim. Acta 119, 31-45. DOI: 10.1016/j.gca.2013.05.028

Xi, D., 2016. Gaseous nitrogen emissions from forest soils. Doctoral dissertation.

Yang, K., Zhu, J.J., Yan, Q.L., Sun, O.J., 2010. Changes in soil P chemistry as affected by conversion of natural secondary forests to larch plantations. For. Ecol. Manage. 260, 422-428. DOI:10.1016/j.foreco.2010.04.038

Zhu, J., Mao, Z., Hu, L., Zhang, J., 2007. Plant diversity of secondary forests in response to anthropogenic disturbance levels in montane regions of Northeastern China. J. For. Res. 12, 403-416. DOI:10.1007/s10310-007-0033-9

827 **Table 1** Estimates of the nitrogen isotope effect ($^{15}\varepsilon$), oxygen isotope effect ($^{18}\varepsilon$) and ratio of O and N isotopic fractionation ($\Delta\delta^{18}O$: $\Delta\delta^{15}N$)

828 during denitrification. Forest-level composite soils collected from 2015 and 2016. Values are means ± 1 SE.

Year	Forest type	Temperature (°C)	O_2	Nitrification inhibitor	Added NO_3^- (μg N g^{-1})	$^{15}\varepsilon$ (‰)	$^{18}\varepsilon$ (‰)	$\Delta\delta^{18}O$:$\Delta\delta^{15}N$	k_1[§]	N
2015	JFL-PF	20	Anaerobic	Yes	20	44.1 ± 1.6	12.7 ± 0.7	0.29 ± 0.07	0.0116	7
	JFL-SF	20	Anaerobic	Yes	20	45.8 ± 2.8	13.0 ± 7.7	0.29 ± 0.02	0.0128	7
	QY-MF	20	Anaerobic	Yes	20	51.4 ± 2.7	16.7 ± 1.0	0.32 ± 0.01	0.0120	7
	QY-LF	20	Anaerobic	Yes	20	40.7 ± 1.8	15.7 ± 1.0	0.38 ± 0.02	0.0110	12
2016	JFL-PF	20	Anaerobic	Yes	20	39.5 ± 8.1	13.6 ± 3.9	0.34 ± 0.07	0.0094	6
	JFL-PF	20	Anaerobic	Yes	10	34.3 ± 3.2	10.7 ± 0.7	0.31 ± 0.03	0.0189	6
	JFL-PF*	20	Anaerobic	Yes	0					
	JFL-PF	20	Anaerobic	No	20	30.8 ± 0.9	12.3 ± 0.5	0.40 ± 0.02	0.0121	6
	JFL-PF	20	Aerobic	Yes	20	43.7 ± 8.7	19.8 ± 4.1	0.43 ± 0.05	0.0016	12
	JFL-PF	20	Aerobic	No	20	52.7 ± 7.7	24.8 ± 4.2	0.46 ± 0.04	0.0014	12
	QY-MF	20	Anaerobic	Yes	20	65.0 ± 2.1	19.5 ± 1.5	0.30 ± 0.02	0.0041	12
	QY-MF	20	Anaerobic	Yes	10	52.7 ± 1.4	15.0 ± 0.9	0.28 ± 0.02	0.0070	12
	QY-MF	20	Anaerobic	Yes	0	45.7 ± 5.8	23.3 ± 1.7	0.47 ± 0.05	0.0050	9
	QY-MF	20	Anaerobic	No	20	57.7 ± 2.2	19.5 ± 1.4	0.34 ± 0.01	0.0045	12
	QY-MF	20	Aerobic	Yes	20	58.3 ± 13.9	39.0 ± 8.2	0.60 ± 0.07	0.0007	12
	QY-MF	20	Aerobic	No	20	64.4 ± 7.5	38.0 ± 3.2	0.56 ± 0.05	0.0008	12

829 * Nitrate isotopes could not be determined due to low nitrate concentration; therefore, isotope fractionation factors were not calculated.

830 [§] $k_1 = \ln([NO_3^-]/[NO_3^-]_{initial})/t$. t is given in hours.

Table 2 Estimates of the nitrogen isotope effect ($^{15}\varepsilon$), oxygen isotope effect ($^{18}\varepsilon$) and ratio of O and N isotopic fractionation ($\Delta\delta^{18}O$: $\Delta\delta^{15}N$) during denitrification. Plot-level composite soils collected from 2016. Values are means ± 1 SE.

	Forest type	Temperature (°C)	O_2	Nitrification inhibitor	Added NO_3^- (μg N g^{-1})	$^{15}\varepsilon$ (‰)	$^{18}\varepsilon$ (‰)	$\Delta\delta^{18}O$:$\Delta\delta^{15}N$	k_1	N
2016	JFL-PF	20	Anaerobic	Yes	20	42.3 ± 2.6	15.3 ± 1.7	0.36 ± 0.05	0.0112	6
	JFL-PF	20	Anaerobic	Yes	20	41.1 ± 6.7	14.2 ± 2.4	0.33 ± 0.07	0.0089	6
	JFL-PF	20	Anaerobic	Yes	20	42.1 ± 3.0	12.1 ± 3.2	0.29 ± 0.07	0.0087	6
	QY-MF	20	Anaerobic	Yes	20	54.0 ±2.7	21.4 ± 1.7	0.40 ± 0.02	0.0045	12
	QY-MF	20	Anaerobic	Yes	20	54.8 ± 2.4	20.0 ± 1.4	0.37 ± 0.01	0.0046	12
	QY-MF	20	Anaerobic	Yes	20	53.3 ± 4.2	21.2 ± 2.7	0.41 ± 0.02	0.0035	12

Table 3 Calculation of N isotope effects during denitrification based on Equations 3 and 4 using $\delta^{15}N$ of N_2O and remaining NO_3^-. Forest-level composite soils were incubated in 2016.

Forest type	Temperature (°C)	Nitrification inhibitor	Added NO_3^- (μg N g^{-1})	Incubation time (day)	$\delta^{15}N$-N_2O	$^{15}\varepsilon$ (‰) according to Equation 4*	$^{15}\varepsilon$ (‰) according to Equation 3**
JFL-PF	20	Yes	20	3	-48.2 ± 0.0		44.0
JFL-PF	20	Yes	20	7	-37.3 ± 0.9		
JFL-PF	20	Yes	20	14	-17.9 ± 0.4	38.4 ± 12.4	
JFL-PF	20	Yes	10	3	-47.0 ± 0.0		50.4
JFL-PF	20	Yes	10	7	-24.0 ± 5.1		
JFL-PF	20	Yes	10	14	-13.0 ± 0.3	64.2 ± 19.9	
JFL-PF	20	Yes	0	3	-21.6 ± 0.5		21.0
JFL-PF	20	Yes	0	7	-16.5 ± 0.1		
JFL-PF	20	Yes	0	14	-2.2 ± 6.2	77.4 ± 93.8	
QY-MF	20	Yes	20	3	-52.6 ± 0.4		55.5
QY-MF	20	Yes	20	7	-42.5 ± 0.1		
QY-MF	20	Yes	20	14	-22.5 ± 0.1	70.4 ± 7.4	
QY-MF	20	Yes	10	3	-48.0 ± 0.3		60.0
QY-MF	20	Yes	10	7	-31.0 ± 5.1		
QY-MF	20	Yes	10	14	-10.0 ± 1.4	65.1 ± 13.6	
QY-MF	20	Yes	0	3	-40.8 ± 0.1		66.6
QY-MF	20	Yes	0	7	-27.1 ± 0.3		
QY-MF	20	Yes	0	14	6.6 ± 0.1	74.0 ± 2.5	

* $^{15}\varepsilon$ was calculated with Equation 4 for 14 days.

** $^{15}\varepsilon$ was calculated with Equation 3 for the first 3 days.

838 **Legends for figures**

839 **Fig. 1** Changes in the concentration of nitrate (NO_3^-) during the incubation of four
840 forest soils (mean value ± 1 standard deviation, n = 3, except n = 2-5 in soil collected
841 in 2015). (A) Forest-level composite soils sampled in 2015; (B, C, D and E)
842 Forest-level composite soils resampled in 2016 under different amendments; (F)
843 Plot-level composite soils sampled in 2016.

844 Note: JFL-PF represents the tropical primary forest; JFL-SF represents the tropical
845 secondary forest; QY-MF represents the temperate mixed forest; QY-LF represents the
846 temperate larch forest.

847

848 **Fig. 2** Nitrogen isotope effect ($^{15}\varepsilon$) and the ratio of O and N isotopic fractionation
849 ($\Delta\delta^{18}O{:}\Delta\delta^{15}N$) during denitrification measured in 2015. (A) NO_3^- $\delta^{15}N$ vs.
850 $\ln([NO_3^-]/[NO_3^-]_{initial})$; (B) NO_3^- $\delta^{18}O$ plotted against the corresponding $\delta^{15}N$.

851 Note: Forest-level composite soils collected in 2015 from two temperate and two
852 tropical forests were incubated at room temperature (approximately 20 °C) with the
853 addition of 20 μg NO_3^--N g^{-1} soil. All P-values are < 0.05 based on linear regressions.

854

855 **Fig. 3** Effects of initial nitrate concentration on the nitrogen isotope effect ($^{15}\varepsilon$) and
856 the ratio of O and N isotopic fractionation ($\Delta\delta^{18}O{:}\ \Delta\delta^{15}N$) during denitrification. (A)
857 NO_3^- $\delta^{15}N$ vs. $\ln([NO_3^-]/[NO_3^-]_{initial})$; (B) NO_3^- $\delta^{18}O$ plotted against corresponding
858 $\delta^{15}N$.

859 Note: Forest-level composite soils collected in 2016 from temperate forests and
860 tropical forests were incubated at room temperature with the addition of 20, 10 or 0
861 μg N g^{-1}. All P-values are < 0.05 based on linear regressions.

862

Fig. 4 Effects of nitrification inhibitor and oxygen on the nitrogen isotope effect ($^{15}\varepsilon$) and the ratio of O and N isotopic fractionation ($\Delta\delta^{18}O$: $\Delta\delta^{15}N$) during denitrification. (A) NO_3^- $\delta^{15}N$ vs. $\ln([NO_3^-]/[NO_3^-]_{initial})$. (B) NO_3^- $\delta^{18}O$ plotted against the corresponding $\delta^{15}N$.

Note: Forest-level composite soils collected in 2016 from the temperate forest and the tropical forest were incubated under anaerobic or aerobic conditions with or without nitrification inhibitor DCD. All P-values are < 0.05 based on linear regressions.

Fig. 5 Nitrogen isotope effect ($^{15}\varepsilon$) and the ratio of O and N isotopic fractionation ($\Delta\delta^{18}O$: $\Delta\delta^{15}N$) during denitrification. (A) NO_3^- $\delta^{15}N$ vs. $\ln([NO_3^-]/[NO_3^-]_{initial})$.; (B) NO_3^- $\delta^{18}O$ plotted against the corresponding $\delta^{15}N$.

Note: Plot-level composite soils collected in 2016 from the temperate forest and the tropical forest were incubated at room temperature (approximately 20 °C) with the addition of 20 μg NO_3^--N g^{-1} soil. All P-values are < 0.05 based on the linear regressions.

Fig. 6 Variations in $^{15}\varepsilon$ of denitrification under different environmental and experimental conditions.

Fig. 7 Relationship between N isotopic effect ($^{15}\varepsilon$) and isotopic rate constant k_1 (first order) in our study in comparison with previous studies.

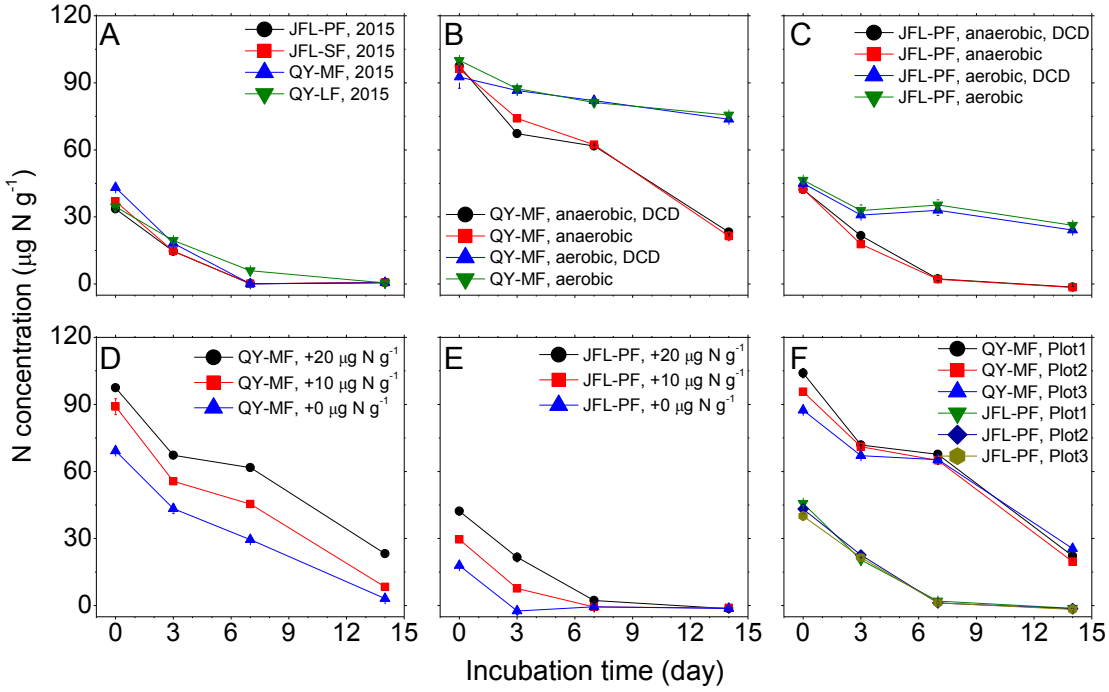
A
JFL-PF, 2015
JFL-SF, 2015
QY-MF, 2015
QY-LF, 2015
B
QY-MF, anaerobic, DCD
QY-MF, anaerobic
QY-MF, aerobic, DCD
QY-MF, aerobic
C
JFL-PF, anaerobic, DCD
JFL-PF, anaerobic
JFL-PF, aerobic, DCD
JFL-PF, aerobic
D
QY-MF, +20 μg N g-1
QY-MF, +10 μg N g-1
QY-MF, +0 μg N g-1
E
JFL-PF, +20 μg N g-1
JFL-PF, +10 μg N g-1
JFL-PF, +0 μg N g-1
F
QY-MF, Plot1
QY-MF, Plot2
QY-MF, Plot3
JFL-PF, Plot1
JFL-PF, Plot2
JFL-PF, Plot3
N concentration (μg N g-1)
Incubation time (day)
0
30
60
90
120
0
3
6
9
12
15

884

885 **Fig. 1**

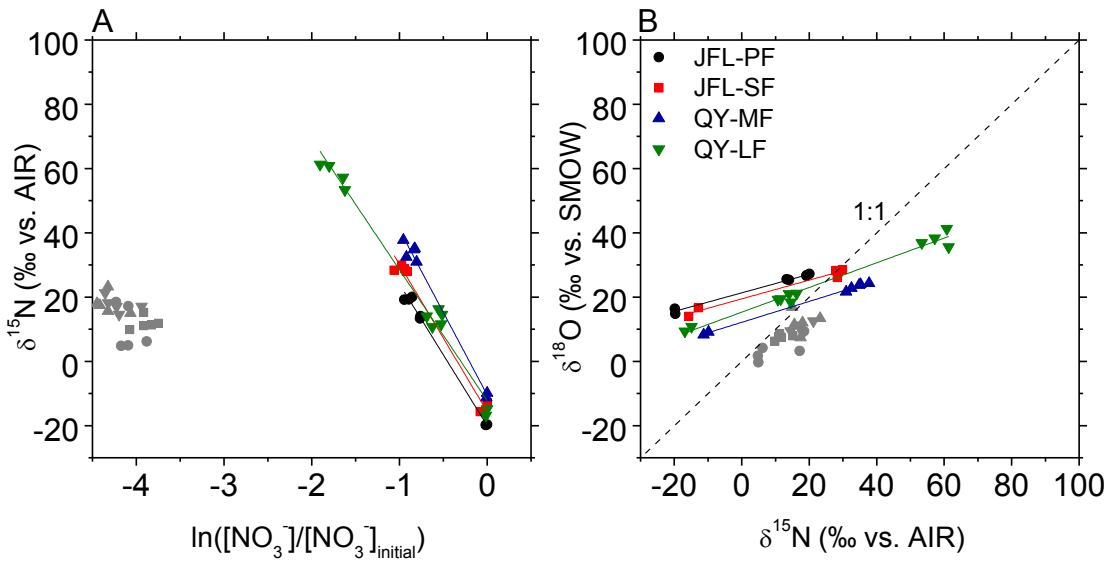
A
B
JFL-PF
JFL-SF
QY-MF
QY-LF
1:1
δ15N (‰ vs. AIR)
ln([NO3-]/[NO3-]initial)
δ18O (‰ vs. SMOW)
δ15N (‰ vs. AIR)

886

887 **Fig. 2**

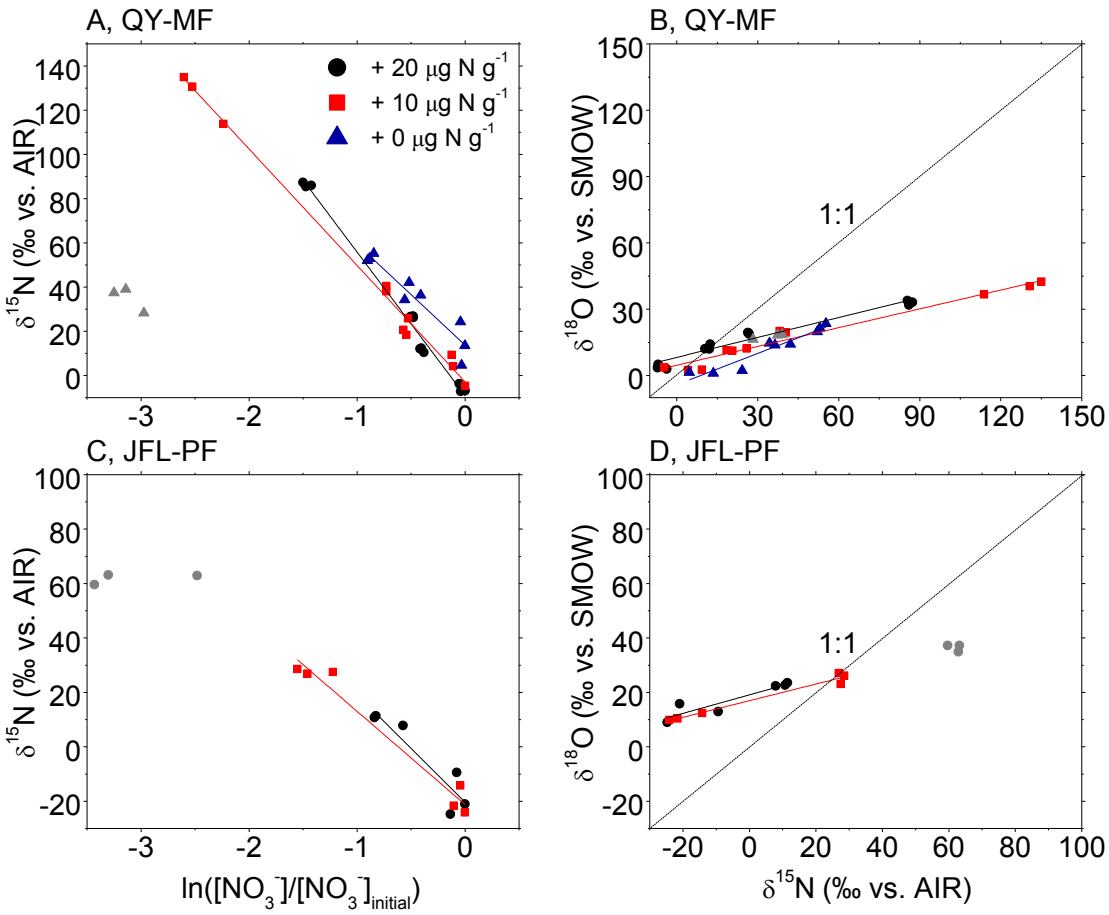
A, QY-MF
+ 20 μg N g-1
+ 10 μg N g-1
+ 0 μg N g-1
δ15N (‰ vs. AIR)
B, QY-MF
1:1
δ18O (‰ vs. SMOW)
C, JFL-PF
δ15N (‰ vs. AIR)
ln([NO3-]/[NO3-]initial)
D, JFL-PF
1:1
δ18O (‰ vs. SMOW)
δ15N (‰ vs. AIR)

888

889 **Fig. 3**

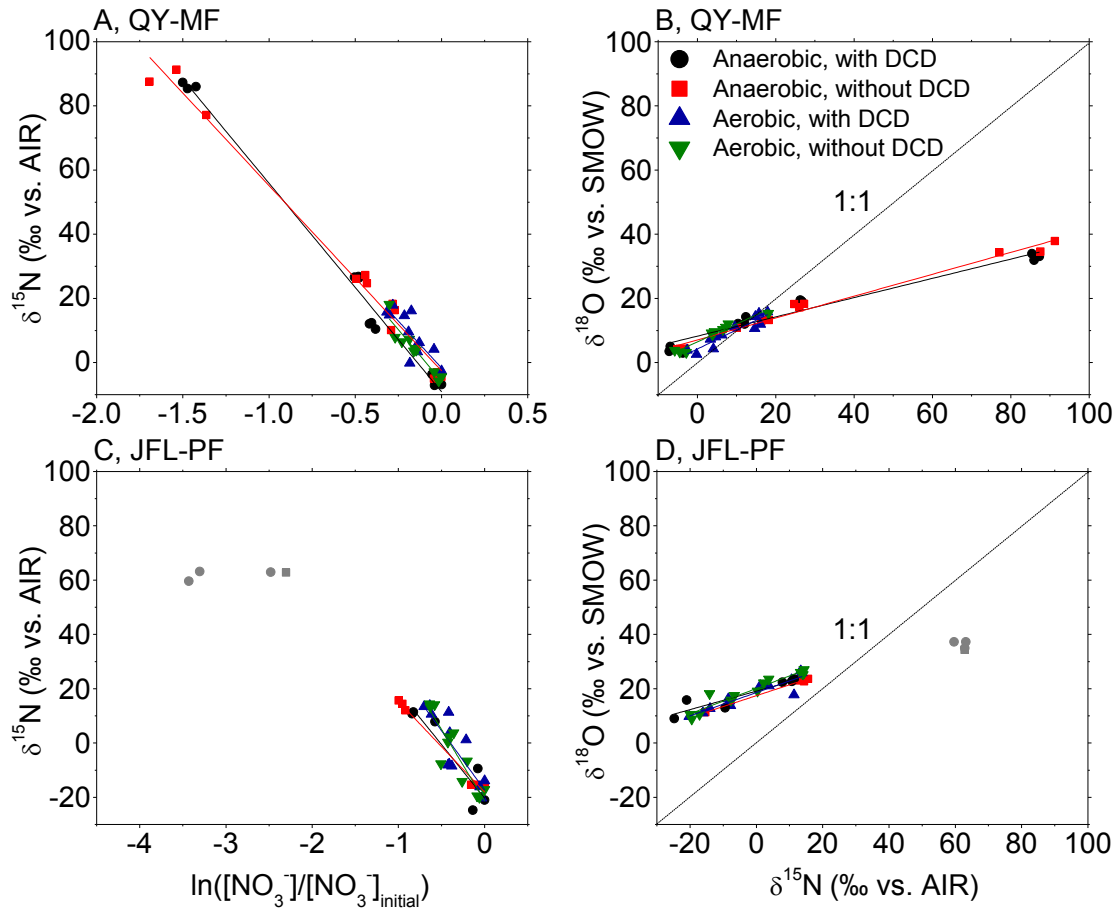
A, QY-MF
B, QY-MF
C, JFL-PF
D, JFL-PF
Anaerobic, with DCD
Anaerobic, without DCD
Aerobic, with DCD
Aerobic, without DCD
1:1
1:1
δ15N (‰ vs. AIR)
δ18O (‰ vs. SMOW)
ln([NO3-]/[NO3-]initial)
δ15N (‰ vs. AIR)

Fig. 4

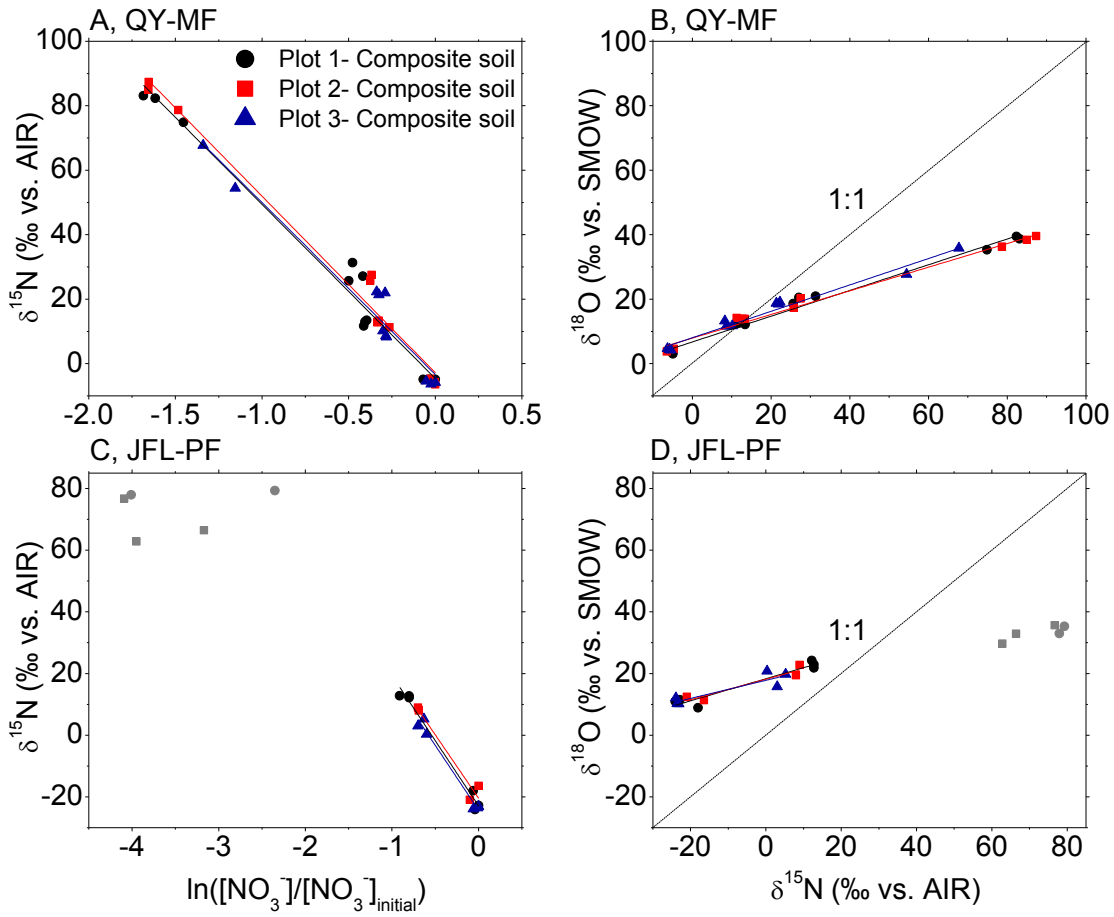
A, QY-MF
Plot 1- Composite soil
Plot 2- Composite soil
Plot 3- Composite soil
δ15N (‰ vs. AIR)
B, QY-MF
1:1
δ18O (‰ vs. SMOW)
C, JFL-PF
δ15N (‰ vs. AIR)
ln([NO3-]/[NO3-]initial)
D, JFL-PF
1:1
δ18O (‰ vs. SMOW)
δ15N (‰ vs. AIR)

892

893 **Fig. 5**

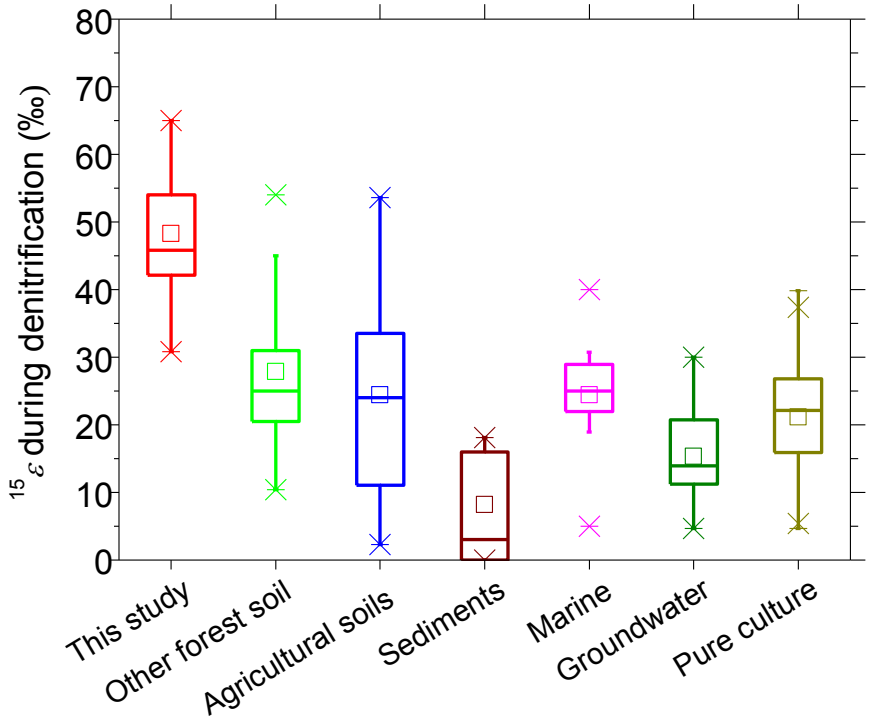

894

895 **Fig. 6**

896

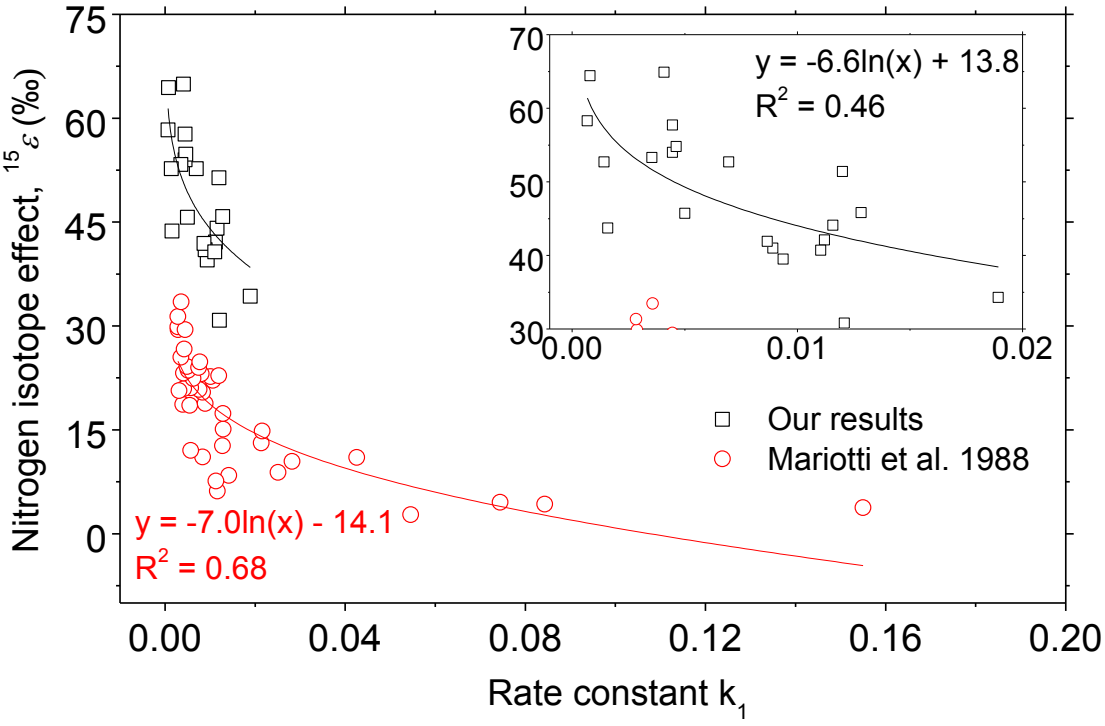
Nitrogen isotope effect, $^{15}\varepsilon$ (‰)
Rate constant k_1
y = -7.0ln(x) - 14.1
R^2 = 0.68
y = -6.6ln(x) + 13.8
R^2 = 0.46
Our results
Mariotti et al. 1988

897

898 **Fig. 7**